Antarct. Meteorite Res., **10**, 335–353, 1997

YAMATO-791093, A METAL-SULFIDE-ENRICHED H-GROUP CHONDRITIC METEORITE TRANSITIONAL TO PRIMITIVE IIE IRONS WITH SILICATE INCLUSIONS

Yukio IKEDA[1], Tizuru YAMAMOTO[1], Hideyasu KOJIMA[2], Naoya IMAE[2], Ping KONG[3], Mitsuru EBIHARA[3] and Martin PRINZ[4]

[1]*Department of Earth Sciences, Ibaraki University, Mito 310*
[2]*National Institute of Polar Research, 9–10, Kaga 1-chome,*
Itabashi-ku, Tokyo 173
[3]*Department of Chemistry, Tokyo Metropolitan University,*
Hachioji-shi, Tokyo 192–03
[4]*Department of Earth and Planetary Sciences, American Museum*
of Natural History, New York, NY 10024, U. S. A.

Abstract: The Y-791093 meteorite consists of volumetrically equal amounts of metal-sulfide-rich and chondritic portions. The chondritic portion is texturally and mineralogically similar to H6 chondrites. The metal-sulfide-rich portion consists mainly of kamacite and troilite; chondritic fragments, including silicate grains and chondrules, are common. The entire assemblage of the metal-sulfide-rich portion is texturally similar to the primitive IIE irons with chondritic inclusions such as Netschaevo and Techado, but richer in sulfide component.

The chondritic, sulfide, and metallic components were analysed by INAA, and compared with average compositions of H chondrites and Netschaevo. The chondritic portion has the same composition as that of average H chondrite. The abundances of siderophile and chalcophile elements in the metal-sulfide-rich portion estimated from the compositions of metallic and sulfide components are similar to those of average H chondrite and Netschaevo, except for higher chalcophiles and a lower Ir content than average H chondrite. The metal-sulfide-rich portion of Y-791093 crystallized from Fe-Ni-S melt produced by shock melting of H chondrites, and Y-791093 was formed by mixing of the Fe-Ni-S melt with H6 chondritic material, near the surface of an H-group chondrite parent body. We conclude that Y-791093 is a transitional member between H chondrites and primitive IIE irons with silicate inclusions.

1. Introduction

Although Y-791093, mass 4.2 g, was previously classified as an H6 chondrite (YANAI and KOJIMA, 1995), it contains a higher abundance of metal than normal H chondrites. Y-791093 consists of metal-sulfide-rich and unmelted H chondritic portions, in roughly equal amounts by volume, and thus is a primitive meteorite transitional between H chondrites and primitive IIE irons with silicate inclusions.

IIE irons were classified by MCCOY (1995) into two types, primitive (Netschaevo, Techado, Watson) and differentiated (Miles, Weekeroo Station, Kodaikanal, Colomera, Elga). Among them Netschaevo (OLSEN and JAROSEWICH, 1971; BILD and WASSON, 1977) and Techado (CASANOVA *et al.*, 1995) are chondrule-bearing meteorites consisting of metal-rich and unmelted chondritic portions. Silicates in the IIE iron group have oxygen isotopic compositions similar to those of H chondrites (CLAYTON *et al.*, 1983; RUBIN *et al.*, 1986), suggesting a genetic relationship. However, further evidence is needed to provide a direct connection between the IIE irons and H chondrites.

Similarly to Y-791093, the Rose City H5 breccia contains more abundant metal than normal H chondrites (MASON and WIIK, 1966), but it is texturally dissimilar to Y-791093 which has no breccia structure. It also contains coarse nodules consisting mainly of metallic Fe-Ni (RUBIN, 1985). The metal is generally considered to have been produced from the chondritic precursor by an impact shock event. Two models for the origin of the metal were proposed. One is a partial melting/fractional crystallization model and the other a vaporization/fractional condensation model (WIDOM *et al.*, 1986; RUBIN, 1995).

In this paper, we describe the mineralogy, petrography and chemistry of Y-791093, and discuss the formation of the metal-sulfide-rich portion and its significance for the origin of IIE irons with silicate inclusions.

2. Analytical Methods

The chemical compositions of the minerals were obtained with a JEOL 733 electron-probe micro-analyser (EPMA at the Department of Earth Sciences, Ibaraki University), using an accelerating voltage of 15 kV and a probe current of 3–5 nA. Compositions were corrected by the BENCE and ALBEE (1986) method for silicates, oxides, and phosphates, and by the standard ZAF method for metal and sulfides.

The areal percentages of the metal (including limonite) and sulfide in the metal-sulfide-rich portion, and the chondritic component, were measured on enlarged photographs of the two surfaces: the cut surface of the meteorite (Fig. 1a) and the polished thin section (Fig. 1b).

Metal, sulfide and silicate components were separated and their major and minor element compositions were obtained by instrumental neutron activation analysis (INAA). The details of the INAA procedures are described in KONG *et al.* (1996). Two samples of each of the components were prepared by the following procedures. A large sample of the meteorite was broken into small pieces by hammer, and chondritic fragments were separated by hand into two fractions; one consists of several large pieces (coarse pieces, 25 mg) and the other of many small pieces (fine pieces, 23.4 mg). Two metal chips, one large (large, 9.2 mg) and one small (small, 3.3 mg), were separated by hand, and limonite adhering to the surface was scraped off by a stainless-steel dental tool. One large sulfide grain, included in metal, was separated by dental tool, and metal adhering to the surface was scraped off. It was broken into fine grains and separated by magnet into two fractions, one magnetic, probably including fine-grained metal (magnetic, 0.3 mg) and one nonmagnetic (nonmagnetic, 0.8 mg).

Fig. 1a. *Photograph of a cut surface of Y-791093. The long dimension of the surface is about 1.5 cm. Abbreviations: Met (metal), Sul (sulfide), and Chond (chondritic portions).*

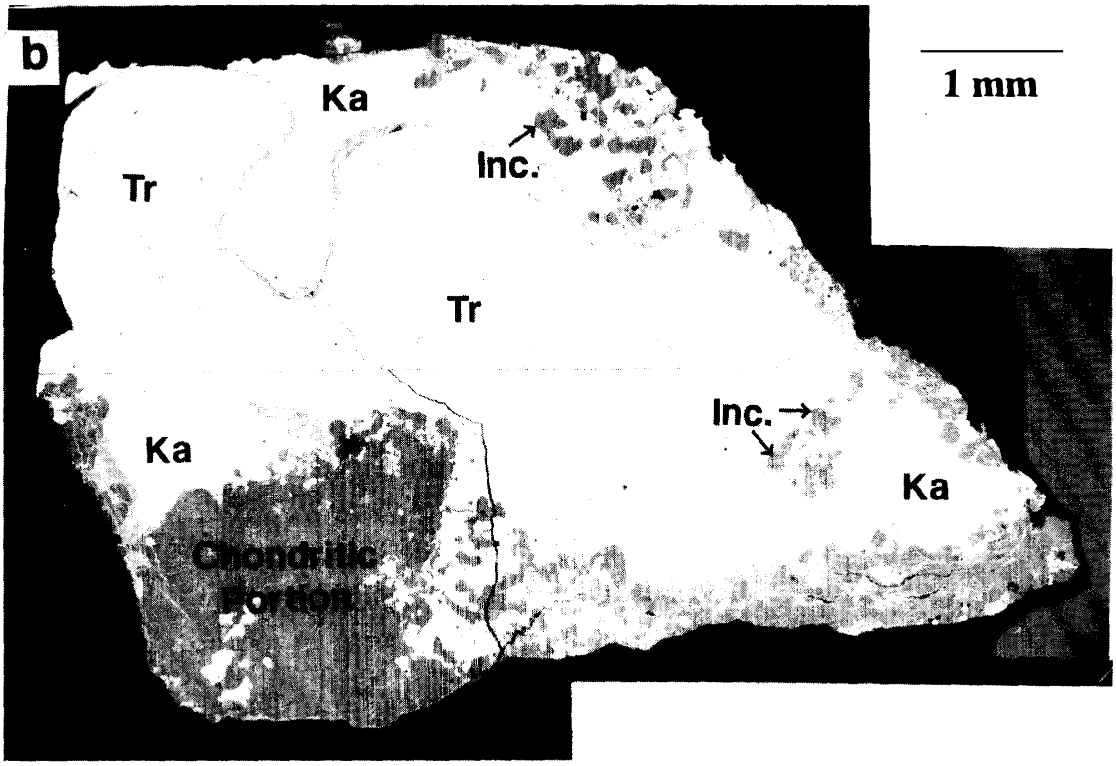

Fig. 1b. *Back-scattered electron (BSE) image of a polished thin section of Y-791093. A chondritic portion is at the lower left. Note that the rims of the kamacite grains are altered to limonite. Tr (troilite), Ka (kamacite), and Inc (silicate inclusions).*

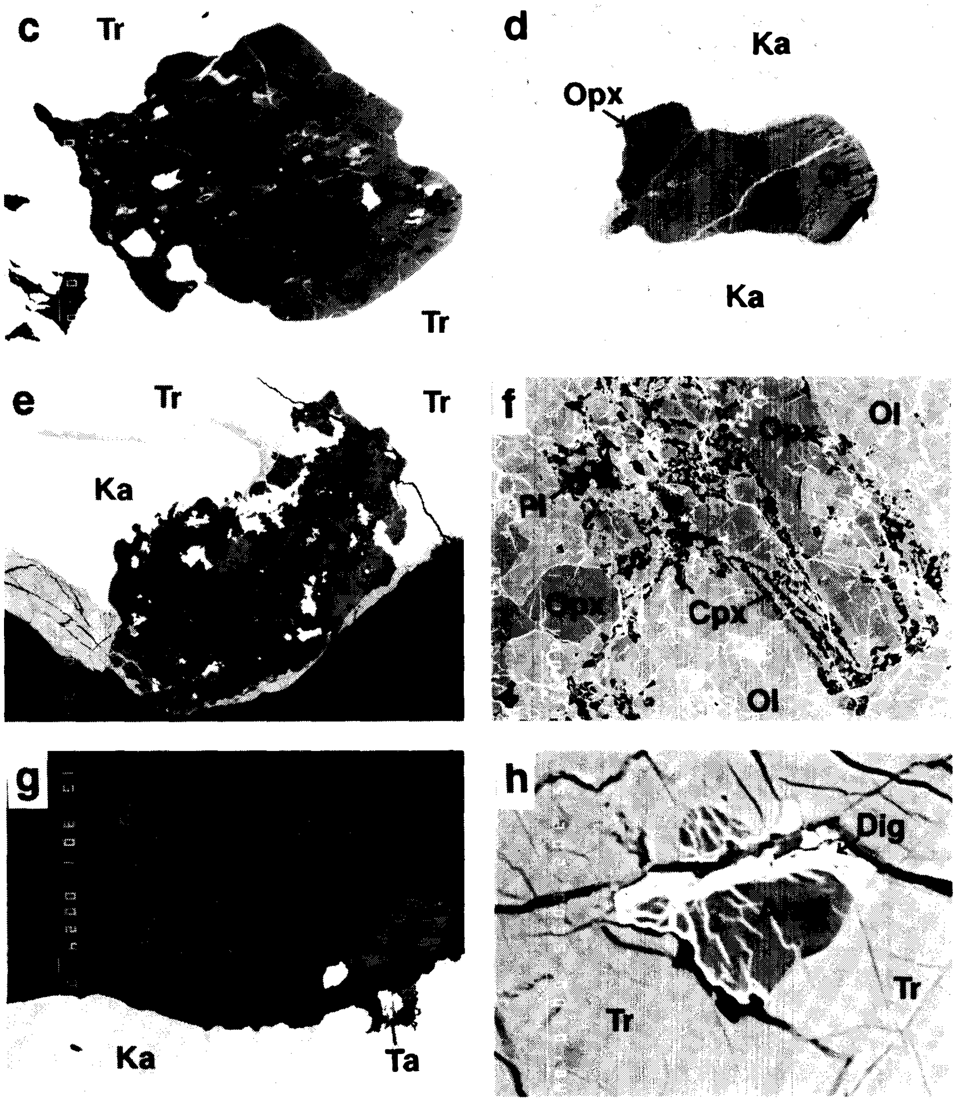

Fig. 1c. BSE image of a barred-olivine chondrule included in a large troilite. Ol (olivine), Opx (orthopyroxene), Pl (plagioclase), and Tr (troilite). The long dimension is 450 μm.

d. BSE image of a silicate inclusion in kamacite (Ka). Abbreviations are the same as those in Fig. 1c. The long dimension is 240 μm.

e. BSE image of a large silicate inclusion which is texturally and mineralogically similar to that of H6 chondrites. Ka (kamacite), Tr (troilite), and Inc (chondritic inclusion). The long dimension is 240 μm.

f. BSE image of a chondritic portion. Light gray is olivine (Ol), dark gray is orthopyroxene (Opx), and black is plagioclase (Pl). High-Ca clinopyroxene (Cpx) occurs as needle crystals in plagioclase and as rims of orthopyroxene in contact with plagioclase. The long dimension is 390 μm.

g. BSE image of pentlandite (Pent) and taenite (Ta) included in a large troilite (Tr). Note that small taenite grains are included in troilite and do not occur in contact with kamacite (Ka). The long dimension is 390 μm.

h. BSE image of alabandite (Alab) and a Cu-bearing sulfide (probably digenite, Dig) included in a large troilite (Tr). The long dimension is 39 μm.

3. Sample Description and Modal Composition

Y-791093 is a heterogeneous mixture of metal-sulfide-rich and chondritic portions (Fig. 1a). The overall texture of the meteorite suggests that a metal-sulfide melt mixed with a monomict chondritic breccia in a reticulate pattern, with some fragments of silicates and chondrules included in the melt (Figs. 1a, b). Metal in the metal-sulfide-rich portion is massive and free from Widmanstätten structure; it contains rounded sulfide inclusions (Fig. 1a). Chondrules (Fig. 1c) and silicates (Figs. 1d and e) occur in both metal and sulfides, and are texturally and mineralogically similar to those in the chondritic portion, indicating they are unmelted chondritic fragments.

The chondritic portion (Fig. 1f) is texturally and mineralogically similar to equilibrated H chondrites. Metal in the chondritic portion is completely replaced by limonite during terrestrial weathering. Plagioclase occurs as coarse (up to 100 μm), well-recrystallized grains which are typical of H6 ordinary chondrites. Therefore, the chondritic portion was probably H6 chondrite. There is no evidence for impact shock in Y-791093.

The modal abundances of the metal and sulfides in the metal-sulfide-rich portion and the chondritic portion, are shown in Table 1. The chondritic portion constitutes about 43.7 vol% (29 wt%) which is higher than in Netschaevo (15 wt%), but lower than in Rose City (about 64 wt%) (Table 1). The sulfide/metal weight ratio of the metal-sulfide-rich portion is about 1/5 (Table 1). This is very large in comparison to that of IIE irons, but is smaller than that in average H chondrite (about 1/3) and Rose City.

Table 1. The modal abundances of Y-791093 (upper table), compared witth the modal compositions of the Netschaevo IIE iron and Rose City H-group chondrite, and the chemical compositions of average H-group chondrite (lower table).

	A cut surface of a piece (100 mm^2)	A polished thin section (30 mm^2)	Average (vol. mean)	Weight percent
Metal	45.0 vol%	30.0 vol%	41.54 vol%	59 wt%
Sulfide	5.2	46.5	14.73	12 wt%
Chondritic portion	49.8	23.5	43.73	29 wt%

	Metal-sulfide portion		Chondritic portion
	Metal	Sulfide	
Y-791093	59 wt%	12 wt%	29 wt%
Netschaevo[1]	85 wt%		15 wt%
(IIE)	(75 vol%)		(25 vol%)
Rose City[2]	27.4 wt%	8.4 wt%	64.2 wt%
(H5 breccia)			(silicates)
Average[3]	17.5 wt%	5.5 wt%	77 wt%
H-group			(silicates)

Data sources: [1]BUCHWALD (1975): [2]MASON and WIIK (1966): [3]HARAMURA *et al.* (1983)

4. Mineralogy

The chondritic portion consists of olivine, orthopyroxene, high-Ca clinopyroxene, plagioclase, chromite, whitlockite, metal (mostly altered to limonite) and sulfide. Olivine and orthopyroxene are dominant and compositionally uniform. Silicates in the metal-sulfide-rich portion are mineralogically and texturally similar to those in the chondritic portion. Representative analyses are given in Table 2.

Metal in the metal-sulfide-rich portion consists of compositionally uniform kamacite; troilite with rare inclusions of pentlandite is the major sulfide mineral (Fig. 1g). Small taenite grains occur in the troilite, in close association with the pentlandite grains (Fig. 1g), but taenite does not occur in kamacite. Alabandite (MnS) is rare; it forms small inclusions in troilites and is closely associated with a Cu-sulfide (probably digenite, Cu_9S_5) (Fig. 1h). Representative compositions of metal and sulfide are given in Table 3.

Table 2. Representative chemical compositions of the minerals in Y-791093 (wt%).

	Ol	Opx	Cpx	Pl	Chm	Wht
SiO_2	39.52	55.97	54.28	64.49	0.00	0.00
TiO_2	0.00	0.17	0.47	0.03	1.33	0.00
Al_2O_3	0.00	0.20	0.57	21.39	6.96	0.00
Cr_2O_3	0.00	0.05	0.65	0.00	57.72	0.00
FeO	17.08	10.77	2.97	0.26	29.77	0.92
MnO	0.37	0.40	0.19	0.00	1.04	0.08
MgO	43.09	30.75	16.45	0.00	2.67	3.66
CaO	0.00	0.59	23.10	2.68	0.01	44.41
Na_2O	0.00	0.02	0.50	9.47	0.00	3.01
K_2O	0.02	0.00	0.00	1.10	0.00	0.05
P_2O_5	–	–	–	–	–	44.87
Total	100.08	98.92	99.17	99.43	99.51	97.00

Abbreviations: Ol (olivine), Opx (orthopyroxene), Cpx (high-Ca clinopyroxene), Pl (plagioclase), Chm (chromite), and Wht (whitlockite). Detection limits for the elements are 0.05–0.1 wt%.

Table 3. Representative chemical compositions of metal and sulfides in Y-791093 (wt%).

	Ka	Ta	Tr	Pent	Alab	Dige
Fe	92.75	41.11	62.49	46.90	2.34	2.19
Co	0.60	0.13	0.11	0.15	0.03	0.06
Ni	6.23	57.85	0.07	18.43	0.03	0.00
Cu	0.04	0.36	0.17	0.09	0.31	70.16
Cr	–	–	–	–	0.01	0.05
Mn	–	–	–	–	59.78	1.14*
P	0.00	0.00	0.00	0.00	0.00	0.07
S	0.00	0.00	36.23	33.75	37.23	23.89
Total	99.62	99.45	99.07	99.32	99.73	97.56

Abbreviations: Ka (kamacite), Ta (taenite), Tr (troilite), Pent (pentlandite), Alab (alabandite, MnS), and Dige (digenite, Cu_9S_5). Detection limits of the elements are 0.05–0.1 wt%.

*: The Mn content of digenite may be due to contamination by surrounding alabandite.

4.1. Olivine and Pyroxene

Olivine (Fo_{80-83}) is the major silicate mineral in the chondritic portion and slicate inclusions in the metal-sulfide-rich portion of the meteorite; it is compositionally similar to olivine in H6 chondrites (Fig. 2). MnO and FeO contents also coincide with those of H6 olivines (Fig. 3).

Low-Ca pyroxene is orthopyroxene, free of exsolution lamellae; its composition($En_{80-84}Wo_{1-2}$) is in the range of H6 orthopyroxenes. High-Ca pyroxene, $En_{45-50}Wo_{43-47}$, is also in the H6 range (Fig. 4). MnO and FeO contents of most pyroxenes are similar to those in H6 chondrites (Fig. 3).

4.2. Plagioclase, Chromite, and Phosphate

Plagioclase ($An_{11-14}Or_{4-8}$) is in the range of H6 plagioclase (Fig. 5). Chromite is compositionally similar to those in H6 chondrite (Figs. 3, 6). Whitlockite occurs in the chondritic portion, but chlorapatite was not observed.

4.3. Metal and Sulfide

The Ni content of kamacite is about 7 wt%, which coincides with the lower limit of H6 kamacites, and the Co content is slightly higher than that in H6 kamacites (Fig. 7). The Ni content of taenite is 56-58 wt% (Fig. 7). No unaltered metal occurs in the chondritic portion, but limonite that was probably formed by replacement of kamacite during terrestrial weathering (Ikeda and Kojima, 1991) is common.

Troilite is the major sulfide in both chondritic and metal-sulfide-rich portions of Y-791093; pentlandite is minor. Sulfide compositions are shown in Fig. 8, together

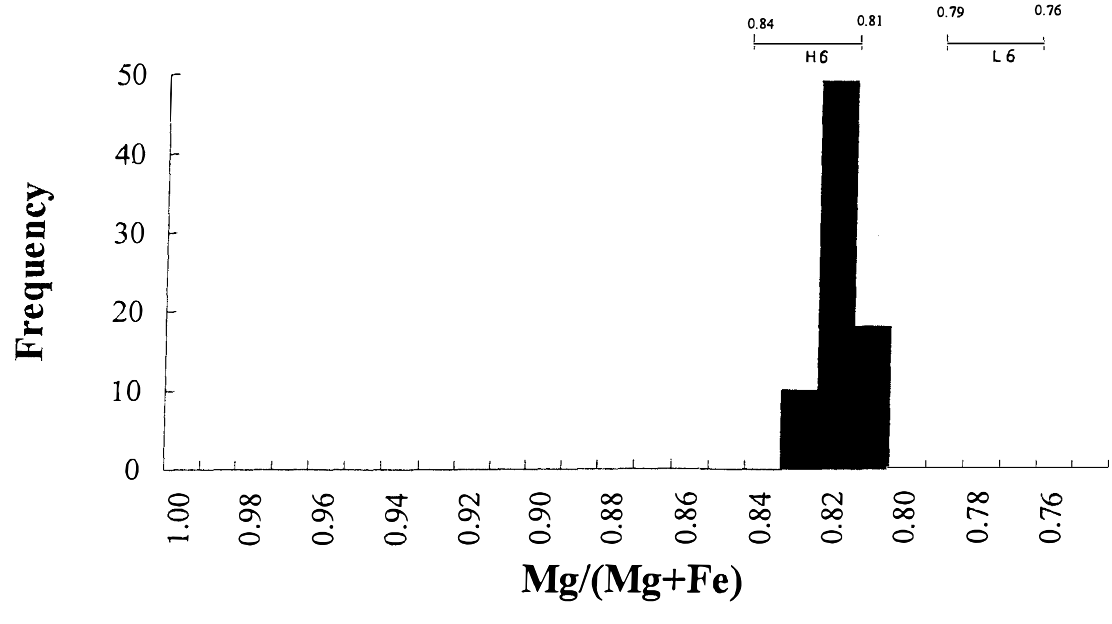

Fig. 2. Frequency diagram of Mg/(Mg+Fe) atomic ratios of olivines in Y-791093. The bars with H6 and L6 are the compositional ranges of olivines in H6 and L6 chondrites, respectively. Note that most of the Y-791093 olivines are within the H6 range.

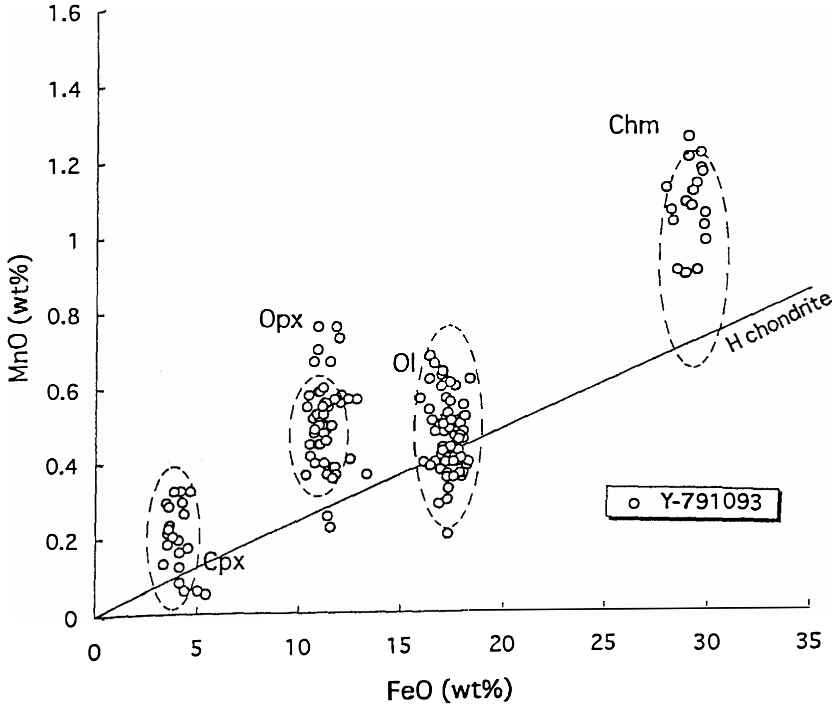

Fig. 3. MnO contents (wt%) of high-Ca clinopyroxene (Cpx), orthopyroxene (Opx), olivine (Ol), and chromite (Chm) plotted against their FeO contents (wt%). The compositional ranges of each of the minerals in H6 chondrites are shown by dash-line ellipsoids. The straight line is the MnO/FeO weight ratio of average H chondrite (Haramura et al., 1983).

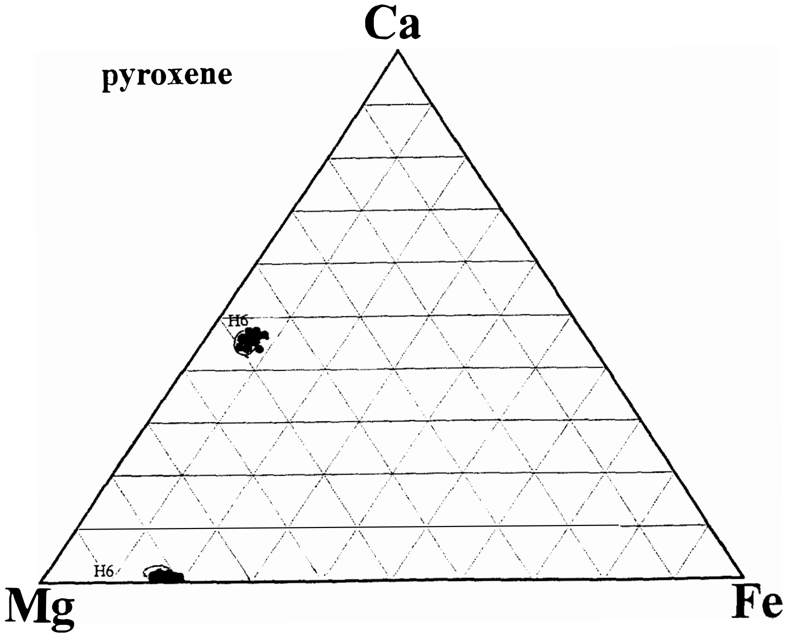

Fig. 4. Ca-Mg-Fe atomic ratios of high-Ca clinopyroxene and orthopyroxene in Y-791093. The compositional ranges of H6 pyroxenes are shown by ellipses.

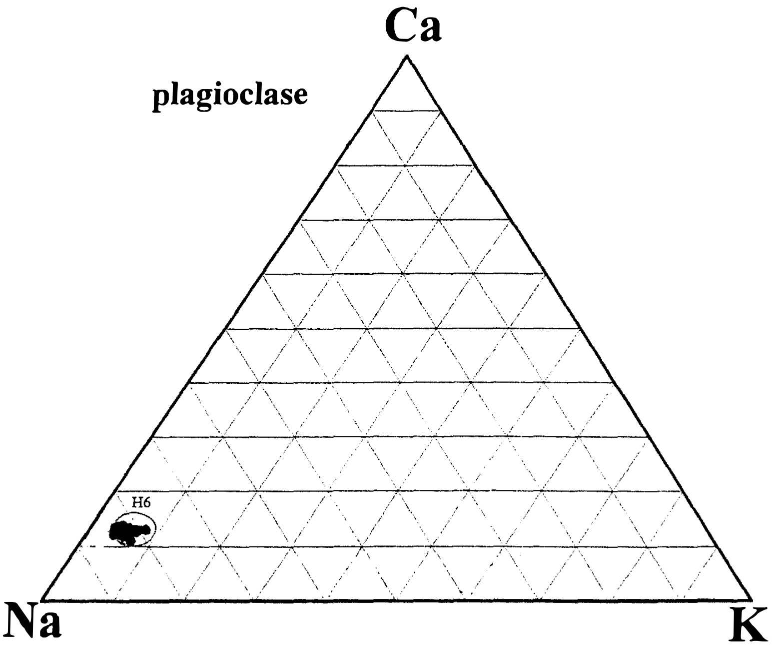

Fig. 5. Ca-Na-K atomic ratios of plagioclase in Y-791093. The 791093 plagioclases are plotted in the compositional range of H6 plagioclases (H6, circle).

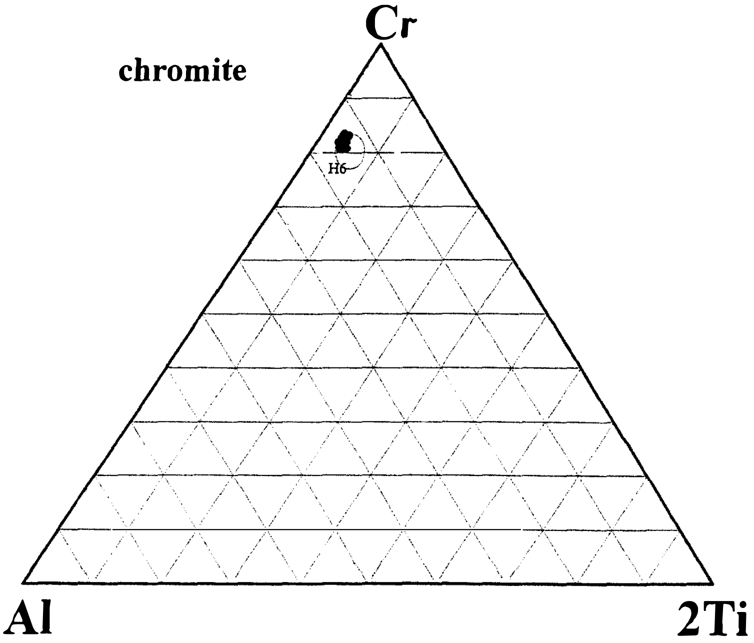

Fig. 6. Cr-Al-2Ti atomic ratios of chromite in Y-791093. The Y-791093 chromites are plotted in the compositional range of H6 chromites (H6, circle). The end components, Cr, Al, and 2Ti, signify the chromite, Al-spinel, and ulvöspinel molecules, respectively.

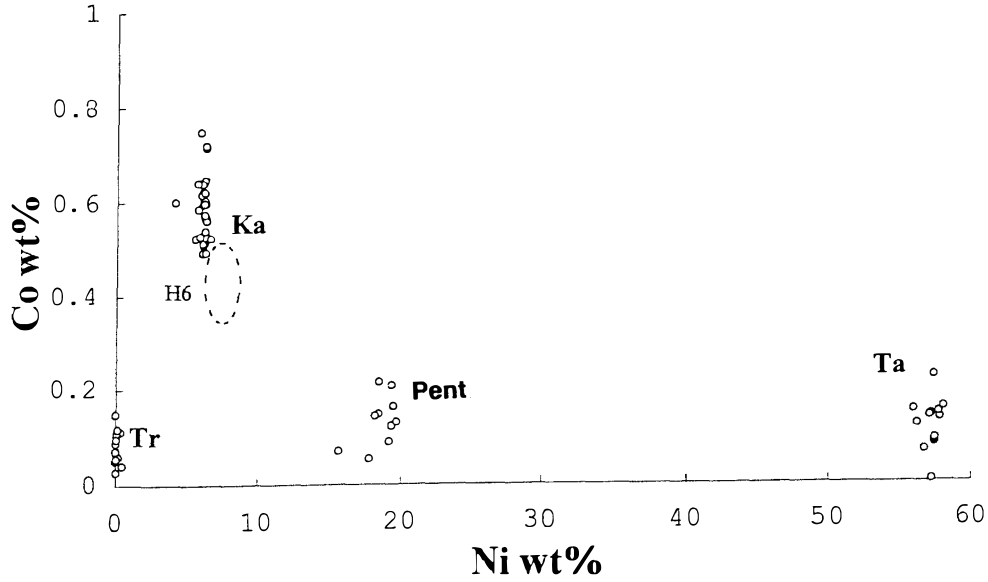

Fig. 7. Co contents (wt%) of kamacite (Ka), taenite (Ta), pentlandite (Pent), and troilite (Tr) in Y-791093. The compositional range of H6 kamacites is shown by a dash-line ellipsoid. Note that the Y-791093 kamacites are slightly enriched in Co in comparison to the H6 kamacites.

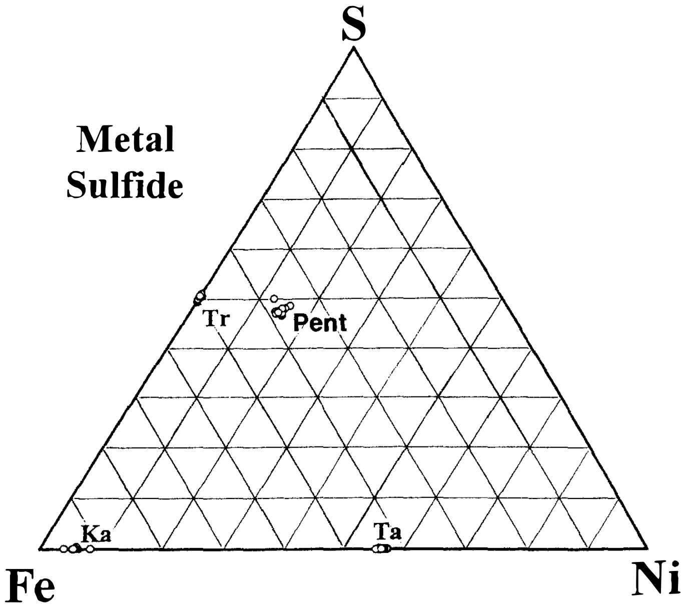

Fig. 8. S-Fe-Ni atomic ratios of kamacite (Ka), taenite (Ta), troilite (Tr), and pentlandite (Pent).

with those of the metal. Pentlandite and taenite in the metal-sulfide-rich portion do not occur in direct contact with kamacite (Fig. 1g). This suggests that pentlandite and taenite may have exsolved from Fe-Ni monosulfide solid solution (later inverted to troilite; Craig *et al.*, 1968) under subsolidus conditions. Alabandite in Y-791093 is depleted in FeS (Table 3); the FeS content is lower than that in E chondrites, indicating that alabandite in Y-791093 formed at temperatures lower than 400°C (SKINNER and LUCE, 1971). An exsolution origin for alabandite and Cu sulfide (probably digenite) (Fig. 1h) is also probable.

5. Chemical Composition

5.1. *The chondritic portion*

Two samples of the chondritic portion analysed by INAA have similar compositions (Table 4, Fig. 9). The abundances of lithophile elements are similar to those in the average H chondrite (WASSON and KALLEMEYN, 1988) and the Netschaevo chondritic portion (BILD and WASSON, 1977), except for Yb, Lu, and Br. Since Yb and Lu measurements have large analytical errors, their high contents may not be certain. The high content of the volatile element Br, compared to that in H chondrites, is consistent with high content of the volatile chalcophile elements such as As, Sb, Se, and Zn (Fig. 9). The siderophile elements are also very similar to those of the average H chondrite (Mo is the only exception). The chondritic portion in Netschaevo has a higher content of siderophile elements than that of the Y-791093 chondritic portion and average H chondrite, suggesting a higher abundance of metal in the chondritic portion of Netschaevo.

5.2. *Metal and sulfide in the metal-sulfide-rich portion*

The INAA results of the metal and sulfide components in the metal-sulfide-rich portion are given in Table 5. Two analysed samples of the metal are compositionally similar, except for Mn (Table 5). The Ni-normalized Os and Ir contents of the metal are lower than in CI and H chondrites, but the other siderophiles are roughly chondritic (Fig. 10). Metal is depleted in chalcophile elements (As is the only exception) (Fig. 10). The lithophile elements V and Cr may be assigned to the silicate inclusions, but Mn is not depleted in spite of the large depletion of the other lithophile elements. Mn content in the large and small metal samples are 77 ppm and 36 ppm, respectively (Table 5), and there is a large difference between the two.

The two fractions of the sulfide component, magnetic and non-magnetic, are compositionally different; the contents of Co, Ni, and As of the magnetic fraction are larg-

Table 4. INAA results for chondritic portions (coarse pieces, 25 mg; fine pieces, 23.4 mg) of Y-791093 (contents in ppm, unless otherwise indicated).

	Al(%)	Sc	Ca(%)	La	Sm	Yb	Lu(ppb)	Mo	V	Cr	Mg(%)	Mn
Coarse	0.91	7.16	1.01	0.39	0.215	0.34	40	2.19	54.7	2760	12.2	2200
Fine	0.85	6.30	0.868	0.24	0.150	0.37	47	3.26	54.8	3180	10.9	1990
Average	0.88	6.73	0.984	0.32	0.183	0.36	44	2.73	54.8	2970	11.6	2095

	Se	Zn	Na	Br	Fe(%)	Co	Ni(%)	Sb(ppb)	As	Au(ppb)	Ir(ppb)	Os(ppb)
Coarse	9.84	45.9	5450	1.82	24.8	786	1.36	86	2.86	193	519	589
Fine	10.8	56.4	5380	1.91	27.9	979	1.65	114	4.05	286	547	496
Average	10.3	51.2	5415	1.87	26.4	883	1.51	100	3.46	240	533	543

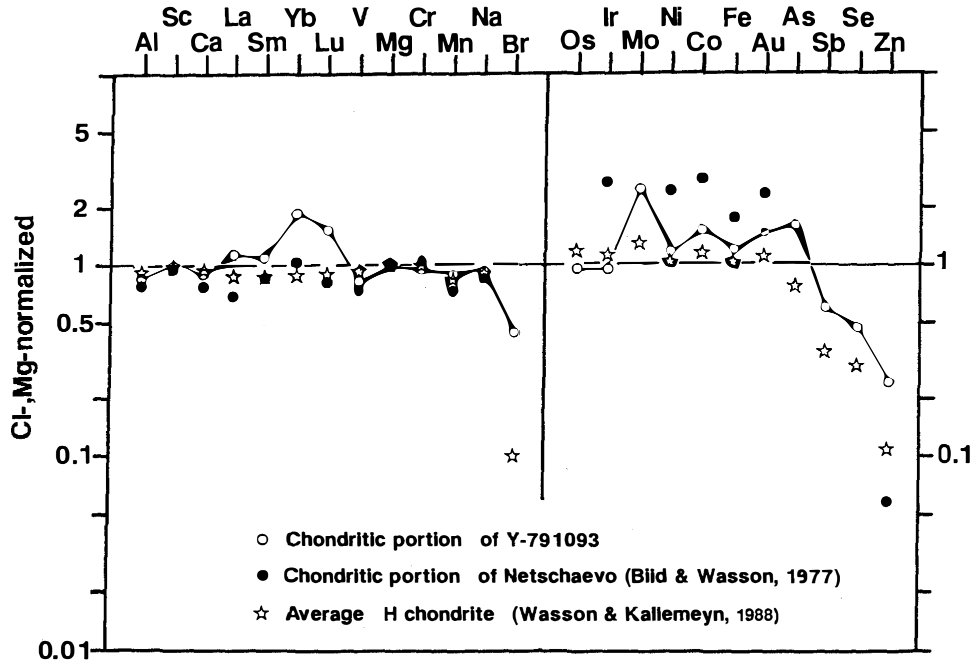

Fig. 9. CI- and Mg-normalized compositions of the Y-791093 chondritic portion compared with the Netschaevo chondritic portion (BILD and WASSON, 1977) and the average H-group chondrite (WASSON and KALLEMEYN, 1988).

Table 5. INAA results for metal (large, 9.2 mg; small, 3.3 mg) and sulfide (magnetic, 0.3 mg; non-magnetic, 0.8 mg) components in the metal-sulfide-predominant portions of Y-791093 (contens in ppm, unless otherwise indicated). S is determined by difference.

	Fe(%)	Co	Ni(%)	Cr	V	W	Mo	Re	Os	Ir
Large metal	92.0	4950	6.97	239	3.6	0.946	5.09	0.140	0.719	0.615
Small metal	92.0	4840	6.59			0.904	4.28	0.126	0.819	0.577
Average (wt. mean)	92.0	4921	6.87	(239)	(3.6)	0.935	4.88	0.136	0.745	0.605
Mag. sulfide	66.2	482	0.498	64						2.04
Non-mag. sulfide	61.4	98.1	0.124	69	5.4		12.1			
Average (wt. mean)	62.7	203	0.226	68	(5.4)		(12.1)			(2.04)

	Ru	Pt	Pd	Au	Cu	Mn	As	Sd	Ga	Se	S(%)
Large metal	(4.09)	3.02	2.97	1.05	134	77	13.1	0.362	11.8		
Small metal		2.94	2.97	1.03	105	36	13.0	0.382	11.8		
Average (wt. mean)	(4.09)	3.00	2.97	1.04	126	66	13.1	0.367	11.8		
Mag. sulfide				0.142	1840	260	0.932	0.676		219	33.0
Non-mag. sulfide				0.067	3470	16	0.163	0.297		178	38.1
Average (wt. mean)				0.087	3025	83	0.373	0.400		189	36.7

er by factors of 4–6 than those of the non-magnetic fraction (Table 5). These high contents are probably due to small metallic inclusions in the magnetic fraction. The Mn content in the magnetic fraction is very high, by a factor of 16.3, compared with the non-magnetic fraction, and may be due to rare alabandite inclusions (Fig. 1h). A weighted mean was calculated to obtain the sulfide component (Table 5), and is shown in Fig. 10.

The composition of the metal-sulfide-rich portion was calculated by using a 5:1 weight ratio of the metal and sulfide components (Table 1), and is shown in Fig. 11. The overall siderophile and chalcophile composition of the metal-sulfide-rich portion is very similar to that of average H chondrite and Netschaevo metallic portion, except for low Ir and slightly high As, Cu, and Sb contents. Although the metal-sulfide-rich portion in Y-791093 has minor contents of V and Cr (Fig. 11), the Mn content is very high in comparison to the lithophiles and reflects the occurrence of alabandite in both the sulfide and metal components.

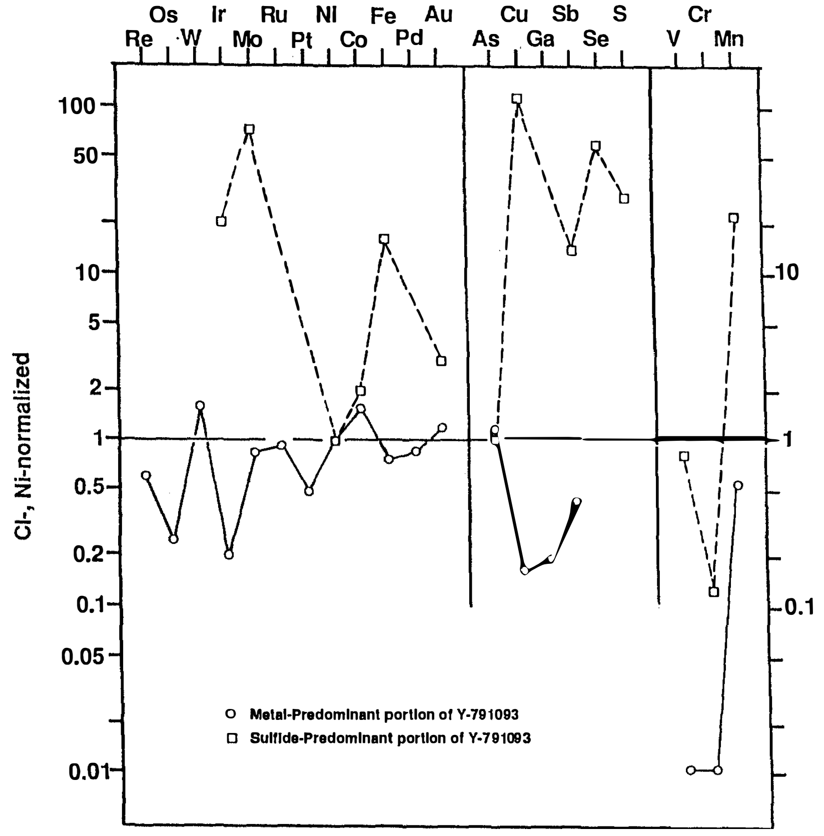

S determined by difference

Fig. 10. CI- and Ni-normalized compositions of the metallic and sulfide components of the metal-sulfide-rich portion of Y-791093.

6. Discussion

6.1. The chondritic portion

The chondritic portion of Y-791093 is texturally, mineralogically and compositionally very similar to H6 chondrites and probably represents an unmelted H6 chon-

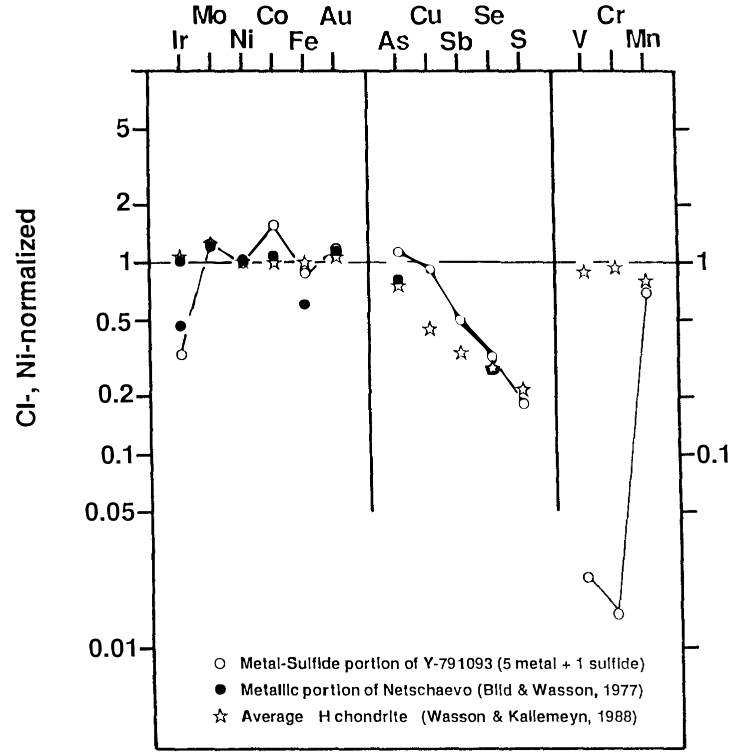

Fig. 11. CI- and Ni-normalized compositions of the metal-sulfide-rich portion of Y-791093, calculated with the weight ratio of metallic and sulfide components of 5:1. The compositions of the Netschaevo metallic portion (BILD and WASSON, 1977, there are two data points for Ir) and the average H-group chondrite (WASSON and KALLEMEYN, 1988) are shown for reference.

drite, although Br, Mo, and volatile chalcophile elements (As, Sb, Se, and Zn) are slightly higher (Fig. 9). Two-pyroxene geothermometry (LINDSLEY and ANDERSEN, 1983) gives equilibrium temperatures of 850–1020°C for the orthopyroxene and high-Ca clinopyroxene pairs in Y-791093, supporting the conclusion that the chondritic portion was originally an H6 chondrite.

There is, however, no taenite in the chondritic portion, which is common in H chondrites. Although limonite is present, it was probably all originally kamacite. If taenite was present, it would have remained unaltered because taenite in the metal-sulfide-rich portion is not altered to limonite. This is consistent with the conclusion of IKEDA and KOJIMA (1991) that taenite is more resistant to terrestrial weathering than kamacite under Antarctic conditions. As discussed in the following sections, the subsolidus assemblage in the metal-sulfide-rich portion may have originally been kamacite and Fe-Ni monosulfide when it formed at high temperature. The mineral assemblage of the H6 chondrite may have changed from kamacite-taenite-troilite to kamacite-monosulfide at a high temperature range when it was mixed with Fe-Ni-S melt. At that time, some fraction of the Mo and volatile chalcophiles may have moved into the chondritic portion from the surrounding Fe-Ni-S melt, resulting in the high contents of these elements (Fig. 9).

6.2. *The metal-sulfide-rich portion*

The metal-sulfide-rich portion makes up about 70 wt% of Y-791093. This is intermediate between that of the Netschaevo IIE iron and the Rose City chondritic breccia. The metal-sulfide-rich portion of all of these meteorites may be the result of variable amounts of Fe-Ni-S melt mixing with H chondrites.

Kamacite is predominant in the metal-sulfide-rich portion of Y-791093, and taenite occurs rarely in the sulfide, in close association with pentlandite. The kamacite is massive and free from Widmanstätten structure, suggesting that it cooled rapidly, preventing its formation.

Troilite is the main sulfide, and the minor phases pentlandite, alabandite, a Cu-sulfide, and probably taenite, may have precipitated from the main sulfide phase which was Fe-Ni monosulfide in the high temperature range.

The overall siderophile and chalcophile composition of the metal-sulfide-rich portion is roughly similar to that of average H chondrite (Fig. 11). However, the Ir content is very low. The Ir/Ni ratio is smaller by a factor of 3 than that of average H chondrite (Fig. 11), indicating that the Fe-Ni-S melt was originally depleted in Ir. The volatile chalcophiles (As, Cu, and Sb) are slightly enriched (1.5–2.5 times) in comparison to average H chondrite (Fig. 11), but Se and S have similar contents. This suggests that although the Fe-Ni-S melt was originally enriched in volatile chalcophiles, including Se and S, some fraction of the Se and S was lost prior to the final consolidation.

The Cu/S weight ratio of average H chondrite is 41×10^{-4} (Wasson and Kallemeyn, 1988) and that of the metal-sulfide-rich portion of Y-791093 is about 100×10^{-4} (calculated from the metal and sulfide components with the weight ratio of 5:1). This suggests that the S content of the metal-sulfide-rich portion was depleted by a factor of 2.5 in comparison to average H chondrite. The original Fe-Ni-S melt may have included more sulfur, and the weight ratio of the metal and sulfide may have been 2:1 prior to sulfur loss, assuming that Cu was not lost from the melt. The weight ratio of metal and sulfide in average H chondrite is 3:1 (Haramura *et al.*, 1983), indicating that a weight ratio of 2:1 for the Y-791093 Fe-Ni-S melt had already lost a small fraction of the metallic component.

As discussed above, the Ir/Ni ratio of the Y-791093 metal is low, and this suggests that the original Fe-Ni-S melt had crystallized and lost Ir-rich metal. The slightly-high Co/Ni ratio (Fig. 10) could be in conflict with the fractional crystallization of metal (Rubin, 1995), but it is small and can be neglected. Therefore, assuming that all of the metal and sulfide in H chondrites was melted by impact shocks, we conclude that the original Fe-Ni-S melt lost a small fraction of Ir-rich metal by fractional crystallization; the residual Fe-Ni-S melt, with a metal/sulfide ratio of 2:1, was mixed with an H6 chondrite. After mixing, some fraction of the volatile chalcophiles in the Fe-Ni-S melt may have been lost to the chondritic portion, and a large amount of Se and S was lost from the Y-791093 system by vaporization.

6.3. *High Mn content of the metal-sulfide-rich portion*

The Mn/Ni ratio of the metal-sulfide-rich portion is exceptionally high (Figs. 10, 11), although the Mn contents of the silicates and oxides in both the chondritic and metal-sulfide-rich portions of Y-791093 are similar to those in normal H chondrites. The high Mn/Ni ratio, which is probably due to inclusions of alabandite mainly in the troilite, is very difficult to explain. During thermal metamorphism of ordinary chondrites, Mn behaves as a lithophile element: it is mainly concentrated in silicates and oxides; as a result, the Mn contents of troilite and metal are very low. If the original Fe-Ni-S melt formed from metal and sulfides in H chondrites, it should not have been enriched in Mn. Nevertheless, some amount of Mn must have moved from the silicates and oxides to the Fe-Ni-S melt during the shock-induced melting. It is likely that H chondrites were wholly melted by an impact event and Mn was redistributed between silicate melt and metal-sulfide melt, resulting in the high Mn content of the Fe-Ni-S melt.

As already discussed, sulfur may have escaped from the sulfur-enriched Fe-Ni-S melt during late-stage crystallization. This may have resulted in an increase in metallic Fe, and a decrease in FeS, of the residual Fe-Ni-S melt. This, in turn, may have resulted in an increase in the concentration of MnS in the sulfide component of the residual Fe-Ni-S melt. The final stage of crystallization may have produced MnS-rich monosulfide which precipitated alabandite at subsolidus temperatures.

6.4. *Origin of the metal-sulfide-rich portion*

Metal nodules and metal veins occur in some shocked but unmelted ordinary chondrites, such as Rose City (WIDOM *et al.*, 1986; RUBIN, 1995). These metal nodules and veins are typically depleted in Ir and S, although W contents are not depleted in comparison to the common siderophiles such as Fe, Co, and Ni. WIDOM *et al.* (1986) attempted to explain these facts by proposing a vaporization/fractional condensation model.

Metal in Y-791093 is depleted in Ir, and W is at the same level as the common siderophiles (Fig. 10). However, the volatile chalcophiles (As, Cu, Sb, Se, and S) of the metal-sulfide-rich portion is slightly enriched in comparison to average H chondrite. This is not consistent with the vaporization/fractional condensation model. Instead, the chemical composition of the metal-sulfide-rich portion in Y-791093 can be explained by a melting/fractional crystallization model, with minor vaporization during crystallization.

This model is schematically illustrated in Fig. 12. (1) H chondrites experienced impact melting near the surface of their parent body. The original Fe-Ni-S melt and silicate melt formed by melting of H chondrite material. The weight ratio of the metal and sulfide components in the Fe-Ni-S melt was about 3:1. (2) The original Fe-Ni-S melt was probably enriched in Mn by its redistribution between the two melts, and the Mn-rich Fe-Ni-S melt separated from the silicate melt. (3) The original Fe-Ni-S melt crystallized Ir-rich metal that resulted in its depletion in Ir and enrichment in S. The Ir-poor and Mn-rich Fe-Ni-S melt had the weight ratio of the metal and sulfide components of about 2:1. (4) The Ir-poor and Mn-rich Fe-Ni-S melt was mixed in a reticulate pattern with a monomict H6 chondrite without melting it. Some silicates and chondrules were trapped by the Fe-Ni-S melt. (5) The Fe-Ni-S melt cooled rapidly, crystallizing kamacite in the early and middle stages of crystallization and both kamacite and Fe-Ni monosulfide in the late stages. (6) Some fraction of Se and S may

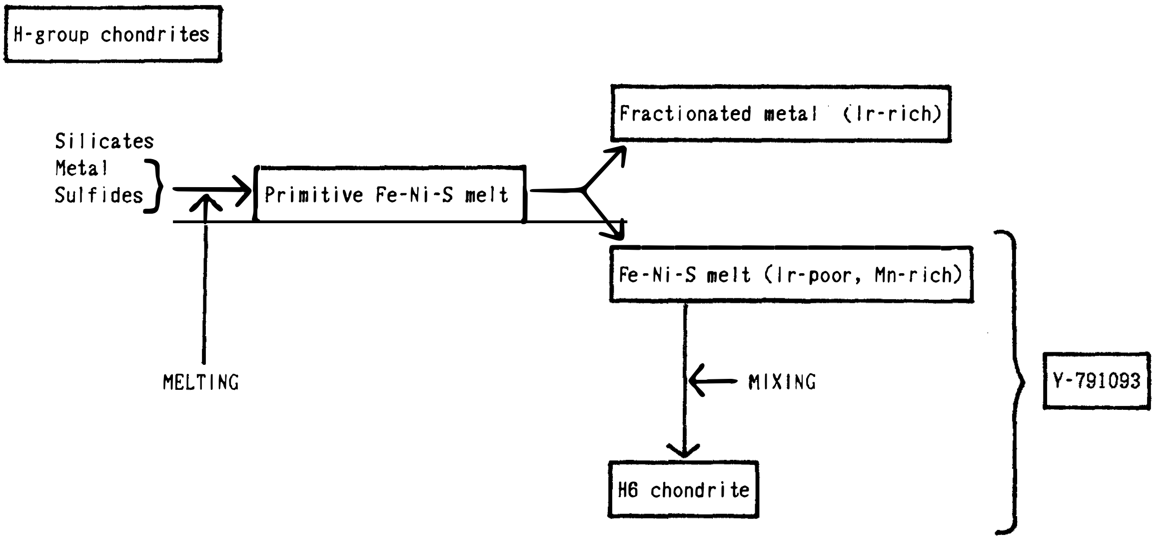

Fig. 12. A schematic figure showing our scenario for the origin of Y-791093. Some H-group chondrite experienced a melting event, probably caused by impact shock on the H-group chondrite parent body, and primitive Fe-Ni-S melt was produced. This melt left behind fractionated metal which was enriched in Ir, and the Ir-poor Fe-Ni-S melt intruded into H6 chondrite, forming the Y-791093 meteorite.

have escaped from the Fe-Ni-S melt during late-stage crystallization of the melt, resulting in a weight ratio of metal and sulfide of 5:1. (7) At the same time, the opaque mineral assemblage of the chondritic portion of Y-791093 changed from kamacite-taenite-troilite to kamacite-monosulfide. The high contents of Br, Mo, and volatile chalcophiles in the chondritic portion (Fig. 9) may have been caused by its impregnation into the chondritic portion from the Fe-Ni-S melt. (8) The Fe-Ni-S melt solidified at a temperature of about 1000°C, around the eutectic point of the Fe-S binary system. (9) At subsolidus temperatures, the metal-sulfide-rich portion consisted mainly of kamacite and monosulfide, and cooled rapidly, resulting in massive kamacite, preventing the formation of Widmanstätten structure. (10) The original Fe-Ni monosulfide exsolved pentlandite, taenite, alabandite, and a Cu-sulfide (probably digenite), and transformed to troilite in the low temperature range.

6.5. Genetic relationship to IIE irons

The close similarity in oxygen isotopic compositions of silicates in IIE irons and H chondrites suggests a genetic relationship (Clayton and Mayeda, 1983; Rubin *et al.*, 1986). However, the origin of IIE irons is controversial, and differing models have been proposed. These include: (1) a silicate melt was trapped in a solidifying iron mass (Wasserburg *et al.*, 1968), (2) metal was mixed with silicates during a shock event (Prinz *et al.*, 1983), (3) IIE irons formed as pools of impact-produced melt near the base of a thick megaregolith (Wasson and Wang, 1986), (4) IIE irons were produced through early mixing and differentiation in a core-mantle environment (McCoy, 1995), (5) IIE iron, free of Widmanstätten structure (Miles), formed as a mixture of Fe-Ni-S melt with silicate melts produced by low degrees of partial melting of H chondrites, caused by impact shocks near the surface of an H chondrite parent body (Ikeda and PRINZ, 1996).

Metal in most IIE irons with silicate inclusions shows Widmanstätten pattern; its cooling rates are estimated to be about 1000°C/Ma at temperatues around 500°C (OLSEN *et al.*, 1994). In addition, OLSEN *et al.* (1994) showed that the younger group of IIE irons (Watson, Kodaikanal, and Netschaevo, with ages of 3.7 Ga) has experienced repeated shock events on the IIE parent body or bodies. These authors concluded that this group of IIE irons formed by near-surface processes. IKEDA and PRINZ (1996) studied the Miles IIE iron and also concluded that Miles was produced at a shallow level on the H chondrite parent body.

The metal-sulfide-rich portion of Y-791093 has silicate and chondrule inclusions which are texturally and mineralogically similar to those in the primitive IIE irons (Netschaevo, Techado, and Watson), except for its sulfide enrichment and lack of Widmanstätten structure. Therefore, Y-791093 may have an intimate genetic relationship with the IIE irons. The data from this study supports the idea that IIE irons were produced near the surface of an H chondrite parent body by impact shock events. The sulfide enrichment in Y-791093 may mean that sulfur loss was smaller than that of the IIE irons because of rapid cooling. The lack of Widmanstätten structure suggests that Y-791093 and Miles were produced at shallow levels.

7. Conclusions

(1) Y-791093 consists of volumetrically equal amounts of metal-sulfide-rich and unmelted H6 chondritic portions.

(2) We suggest that the metal-sulfide-rich portion formed as a result of impact melting of the metal and sulfide in H chondrite material. The original Fe-Ni-S melt produced during this process had a chondritic composition, except for its high Mn content; it crystallized Ir-rich metal that was lost prior to the mixing of the Fe-Ni-S melt with H6 chondritic material.

(3) We infer that the mixing of the metal-sulfide melt and unmelted H6 chondrite took place near the surface of an H chondrite parent body. Some fraction of the S and Se in the melt was lost from the system due to vaporization during crystallization.

(4) The metal-sulfide-rich portion of Y-791093 is texturally, mineralogically, and compositionally similar to the primitive IIE irons with chondritic inclusions such as Netschaevo and Techado, suggesting that primitive IIE irons were produced in a manner similar to that of Y-791093.

Acknowledgments

We thank Dr. A.N. KROT for improving our manuscript. This study was partially supported by funds from JSPS grant, Japan-Korea Co-operative Study on Antarctic Meteorites (to Y. IKEDA), and from NASA grant NAGW 34-90 (to M. PRINZ).

References

BENCE, A. E. and ALBEE, A. L. (1968): Empirical correction factors for the electron microanalysis of silicates and oxides. J. Geol., **76**, 382–403.

BILD, R. and WASSON, J. T. (1977): Netschaevo: A new class of chondritic meteorite. Science, **197**, 58–62.

BUCHWALD V. F. (1975): Handbook of Iron Meteorites. Berkeley, Univ. California Press.

CASANOVA, I., GRAF, T. and MARTI, K. (1995): Discovery of an unmelted H-chondrite inclusion in an iron meteorite. Science, **68**, 540–542.

CLAYTON, R. N., MAYEDA, T. K., OLSEN, E. J. and PRINZ, M. (1983): Oxygen isotope relationships in iron meteorites. Earth Planet. Sci. Lett., **65**, 229–232.

CRAIG, J. R., NALDRETT, A. J. and KULLERUD, G. (1968): The Fe-Ni-S system: 400°C isothermal diagram. Carnegie Inst. Washington, Yearb., **66**, 440–441.

HARAMURA, H., KUSHIRO, I. and YANAI, K. (1983): Chemical compositions of Antarctic meteorites I. Mem. Natl Inst. Polar Res., Spec. Issue, **30**, 109–121.

IKEDA, Y. and KOJIMA, H. (1991): Terrestrial alteration of Fe-Ni metals in Antarctic ordinary chondrites and the relationship to their terrestrial ages. Proc. NIPR Symp. Antarct. Meteorites, **4**, 307–318.

IKEDA, Y. and PRINZ, M. (1996): Petrology of silicate inclusions in the Miles IIE iron. Proc. NIPR Symp. Antarct. Meteorites, **9**, 143–173.

KONG, P., EBIHARA, M. and NAKAHARA, H. (1996): Precise determination of 18 siderophile elements including all platinum group elements for chondritic metals and iron meteorites by instrumental neutron activation. Anal. Chem., **68**, 4130–4134.

LINDSLEY, D. H. and ANDERSEN, D. J. (1983): Two pyroxene geothermometer. Proc. Lunar Planet. Sci. Conf., 13th, Pt. 2, A887–A906 (J. Geophys. Res., **88** suppl.).

MASON, B. and WIIK, H. B. (1966): Meteorites. Am. Mus. Novit., **2272**, 14–18.

MCCOY, T. J. (1995): Silicate-bearing IIE irons: Early mixing and differentiation in a core-mantle environment and shock resetting of ages. Meteoritics, **30**, 542–543.

OLSEN, E. and JAROSEWICH, E. (1971): Chondrules: First occurrence in an iron meteorite. Science **174**, 583–585.

OLSEN, E., DAVIS, A., CLARKE, R.S., SCHULTZ, L., WEBER, H. W., CLAYTON, R., MAYEDA, T., JAROSEWICH, E., SYLVESTER, P., GROSSMAN, L., WANG, M. S., LIPSCHUTZ, M. E., STEELE, I. M. and SCHWADE, J. (1994): Watson: A new link in the IIE iron chain. Meteoritics, **29**, 200–213.

PRINZ, M., NEHRU, C., DELANEY, J., WEISBERG, M. and OLSEN, E. (1983): Globular silicate inclusions in IIE irons and Sombrerete: Highly fractionated minimum melts. Lunar and Planetary Science XIV. Houston, Lunar Planet. Inst., 616–617.

RUBIN, A. E. (1985): Impact melt products of chondritic material. Rev. Geophys., **23**, 277–300.

RUBIN, A. E. (1995): Fractionation of refractory siderophile elements in metal from the Rose City meteorite. Meteoritics, **30**, 412–417.

RUBIN, A. E., JERDE, E., ZONG, P., WASSON, J. T., WESTCOTT, J. W., MAYEDA, T. K. and CLAYTON, R. N. (1986): Properties of the Guin ungrouped iron meteorite: The origin of Guin and of group-IIE irons. Earth Planet. Sci. Lett., **76**, 209–226.

SKINNER, B. J. and LUCE, F. D. (1971): Solid solutions of the type (Ca, Mg, Mn, Fe)S and their use as geothermometers for the enstatite chondrites. Am. Mineral., **56**, 1269–1296.

WASSERBURG, G. J., SANZ, H. G. and BENCE, A. E. (1968): Potassium-feldspar phenocrysts in the surface of Colomera, an iron meteorite. Science, **161**, 684–687.

WASSON, J. T. and KALLEMEYN, G. W. (1988): Compositions of chondrites. Philos. Trans. R. Soc. London, **A325**, 535–544.

WASSON, J. T. and WANG, J. (1986): A nonmagmatic origin of group-IIE iron meteorites. Geochim. Cosmochim. Acta, **50**, 725–732.

WIDOM, E., RUBIN, A. E. and WASSON, J. T. (1986): Composition and formation of metal nodules and veins in ordinary chondrites. Geochim. Cosmochim. Acta, **50**, 1989–1995.

YANAI, K. and KOJIMA, H. comp. (1995): Catalog of the Antarctic Meteorites. Tokyo, Natl Inst. Polar Res., 230p.

(*Received August 27, 1996; Revised manuscript accepted December 9, 1996*)